To link to this article : DOI:10.1016/j.ijheatmasstransfer.2010.05.032
URL : http://dx.doi.org/10.1016/j.ijheatmasstransfer.2010.05.032

Equivalence between volume averaging and moments matching techniques for mass transport models in porous media

Yohan Davit [a], Michel Quintard [a,b], Gérald Debenest [a,b,c,*]

[a] Université de Toulouse, INPT, UPS, IMFT (Institut de Mécanique des Fluides de Toulouse), Allée Camille Soula, F-31400 Toulouse, France
[b] CNRS, IMFT, F-31400 Toulouse, France
[c] Ecolab UMR 5245 (INP-ENSAT, UPS, CNRS), Equipe ECOGEN, Av. de l'Agrobiopole, BP 32607 Auzeville Tolosane, 31326 Castanet Tolosan Cedex, France

Keywords:
Porous media
Non-equilibrium
Two-equation model
Moments
Time-asymptotic
Volume averaging

A B S T R A C T

This paper deals with local non-equilibrium models for mass transport in dual-phase and dual-region porous media. The first contribution of this study is to formally prove that the time-asymptotic moments matching method applied to two-equation models is equivalent to a fundamental deterministic perturbation decomposition proposed in Quintard et al. (2001) [1] for mass transport and in Moyne et al. (2000) [2] for heat transfer. Both theories lead to the same one-equation local non-equilibrium model. It has very broad practical and theoretical implications because (1) these models are widely employed in hydrology and chemical engineering and (2) it indicates that the concepts of volume averaging with closure and of matching spatial moments are equivalent in the one-equation non-equilibrium case. This work also aims to clarify the approximations that are made during the upscaling process by establishing the domains of validity of each model, for the mobile–immobile situation, using both a fundamental analysis and numerical simulations. In particular, it is demonstrated, once again, that the local mass equilibrium assumptions must be used very carefully.

1. Introduction

In this paper, we investigate the behavior of widely used models, especially in subsurface hydrology, for describing the transport of a tracer through dual-phase and dual-region porous media similar to those presented in Fig. 1. At the microscopic scale (pore-scale or Darcy-scale in this article), these two systems are usually thought as two continua, in which advection and Fickian diffusion/dispersion are dominant. Upscaling mass balanced equations from the pore-scale to the Darcy-scale in a dual-phase porous medium is, mathematically speaking, equivalent to upscaling from the Darcy-scale to the large-scale in a dual-region porous medium. Hence, in this work, we consider a general framework defined by the mathematical structure of the boundary-value problem at the small scale rather than by the scale itself and the corresponding physical phenomena.

A general solution to the dispersion problem at the macroscopic scale exhibits time and spatial convolutions (non-locality) [3–8]. Direct Numerical Simulations can be used to get an accurate response, but it is not often tractable for most of porous systems because of the complexity involved. Degraded models, but still rather accurate if one is concerned with the estimate of the flux exchanged between the different phases/regions, can be derived under the form of mixed models for mobile/immobile systems, i.e. systems with high diffusivity contrast and no advection in the low diffusivity phase/region [9–12]. In many practical applications, relevant constraints can be formulated concerning characteristic times and length scales [13], that is, when the different length scales of the system are separated by several orders of magnitude, non-local effects tend to disappear. One way of describing the transport while conserving partly the convolutions effects consists in using a two-equation quasi-stationary model (Eqs. (1) and (2)) involving two macroscopic concentrations, one for each phase/region γ and ω. Herein, the bracket notation is used as a reminder that concentrations appearing in the macroscopic equations are defined in a volume averaged sense. ε_i is the volume fraction of the *i-phase/region* and the star notation refers to the model effective parameters. In particular, α^{**} is a first order mass exchange coefficient.

Two-equation model:

$$\varepsilon_\gamma \partial_t \langle c_\gamma \rangle^\gamma + \mathbf{V}^{**}_{\gamma\gamma} \cdot \nabla \langle c_\gamma \rangle^\gamma + \mathbf{V}^{**}_{\gamma\omega} \cdot \nabla \langle c_\omega \rangle^\omega = \nabla \cdot \left\{ \mathbf{D}^{**}_{\gamma\gamma} \cdot \nabla \langle c_\gamma \rangle^\gamma \right\} + \nabla \cdot \left\{ \mathbf{D}^{**}_{\gamma\omega} \cdot \nabla \langle c_\omega \rangle^\omega \right\} - \alpha^{**} \left\{ \langle c_\gamma \rangle^\gamma - \langle c_\omega \rangle^\omega \right\} \quad (1)$$

* Corresponding author at: Université de Toulouse, INPT, UPS, IMFT (Institut de Mécanique des Fluides de Toulouse), Allée Camille Soula, F-31400 Toulouse, France.
E-mail addresses: davit@cict.fr (Y. Davit), quintard@imft.fr (M. Quintard), debenest@imft.fr (G. Debenest).

Nomenclature

Roman symbols

A_{ij}	boundary area between the *i-phase/region* and the *j-phase/region* (m^2)
$\mathbf{b}_{ij}$	two-equation model closure vectorial variables (m)
$\mathbf{b}_i$	one-equation special decomposition model closure vectorial variables (m)
$\mathbf{b}_{\mathrm{I}i}$	$\mathbf{b}_i$ part I decomposition (m)
$b_{\mathrm{II}i}$	$\mathbf{b}_i$ part II decomposition (–)
$\mathbf{B}_i$	one-equation time-asymptotic model closure vectorial variables (m)
$\mathbf{B}_{\mathrm{I}i}$	$\mathbf{B}_i$ part I decomposition (m)
$B_{\mathrm{II}i}$	$\mathbf{B}_i$ part II decomposition (–)
c_i	concentration at the microscopic scale in the *i-phase/region* (mol m^{-3})
$\langle c_i \rangle$	superficial average of c_i (mol m^{-3})
$\langle c_i \rangle^i$	intrinsic average of c_i (mol m^{-3})
$\langle c \rangle^{\gamma\omega}$	weighted average concentration (mol m^{-3})
$\tilde{c}_i$	solute concentration standard deviation in the *i-phase/region* (mol m^{-3})
$\hat{c}_i$	solute concentration special deviation in the *i-phase/region* (mol m^{-3})
$\mathbf{D}_i$	diffusion/dispersion tensor at the microscopic scale in the *i-phase/region* ($m^2\ s^{-1}$)
$\mathbf{D}^{equ}$	one-equation local mass equilibrium dispersion tensor ($m^2\ s^{-1}$)
$\mathbf{D}^{\infty}$	one-equation time-asymptotic model dispersion tensor ($m^2\ s^{-1}$)
$\mathbf{D}^{*}$	one-equation special decomposition model dispersion tensor ($m^2\ s^{-1}$)
$\mathbf{D}_{ij}$	two-equation model macroscopic dispersion tensors ($m^2\ s^{-1}$)
$\mathbf{d}_\omega - \mathbf{d}_\gamma$	two-equation model macroscopic part of velocity ($m\ s^{-1}$)
$\mathbf{j}_\phi$	flux tensor of the quantity ϕ (mol $m^{-2}\ s^{-1}$)
V	volume of a REV (m^3)
l_i	characteristic length of the *i-phase* (m)
L	characteristic length of the *field-scale* (m)
$\mathbf{n}_{ij}$	normal to A_{ij} pointing from i to j (–)
Pe	microscopic Péclet number (–)
R_0	radius of a REV (m)
r_i	two-equation model closure scalar variables (–)
$r_{\mathrm{II}i}$	r_i part II decomposition (m)
$\mathbf{U}^{*}$	macroscopic velocity contrast ($m\ s^{-1}$)
V_i	volume of the *i-phase* within a REV (m^3)
$\mathbf{v}_i$	velocity at the microscopic scale in the *i-phase/region* ($m\ s^{-1}$)
$\langle \mathbf{v}_i \rangle$	superficial average of $\mathbf{v}_i$ ($m\ s^{-1}$)
$\langle \mathbf{v}_i \rangle^i$	intrinsic average of $\mathbf{v}_i$ ($m\ s^{-1}$)
$\tilde{\mathbf{v}}_i$	velocity standard deviation in the *i-phase/region* ($m\ s^{-1}$)
$\mathbf{V}_{ij}$	two-equation model macroscopic velocities ($m\ s^{-1}$)
$\mathbf{V}$	one-equation local mass equilibrium, time-asymptotic and special decomposition models macroscopic velocity ($m\ s^{-1}$)

Greek symbols

α^{**}	two-equation model macroscopic exchange coefficient (s^{-1})
$\boldsymbol{\beta}^{*}$	one-equation time-asymptotic model macroscopic $\mathbf{B}_l$ tensorial flux ($m^2\ s^{-1}$)
ε_i	*i-phase/region* porosity (–)
$\boldsymbol{\Phi}_{\mathrm{I}i}$	*i-phase/region* problem type I solution (m)
$\Phi_{\mathrm{II}i}$	*i-phase/region* problem type II solution (–)

Subscript and superscript

i, j	indexes for γ or ω (–)

$$\begin{aligned}\varepsilon_\omega \partial_t \langle c_\omega \rangle^\omega &+ \mathbf{V}^{**}_{\omega\gamma} \cdot \nabla \langle c_\gamma \rangle^\gamma + \mathbf{V}^{**}_{\omega\omega} \cdot \nabla \langle c_\omega \rangle^\omega \\ &= \nabla \cdot \left\{ \mathbf{D}^{**}_{\omega\gamma} \cdot \nabla \langle c_\gamma \rangle^\gamma \right\} + \nabla \cdot \left\{ \mathbf{D}^{**}_{\omega\omega} \cdot \nabla \langle c_\omega \rangle^\omega \right\} \\ &\quad - \alpha^{**} \left\{ \langle c_\omega \rangle^\omega - \langle c_\gamma \rangle^\gamma \right\} \end{aligned} \tag{2}$$

Since this model showed good agreement in numerous works with both numerical computations and experimental data [14–18], it has been broadly used to explore some physical aspects of the problem. In particular, two very different situations leading to simple Fickian dispersion have been identified [19,1,20]. On the one hand, when the macroscopic concentration in one-phase/region can be expressed as a thermodynamic function of the concentration in the other phase/region, the situation is called local mass equilibrium [1] and a one-equation model (Eq. (3)) represents a reasonable approximation of the mass transport problem.

One-equation local mass equilibrium model:

$$(\varepsilon_\gamma + \varepsilon_\omega) \partial_t \langle c \rangle^{\gamma\omega} + \mathbf{V} \cdot \nabla \langle c \rangle^{\gamma\omega} = \nabla \cdot \left\{ \mathbf{D}^{equ} \cdot \nabla \langle c \rangle^{\gamma\omega} \right\} \tag{3}$$

where

$$\langle c \rangle^{\gamma\omega} = \frac{\varepsilon_\gamma}{\varepsilon_\gamma + \varepsilon_\omega} \langle c_\gamma \rangle^\gamma + \frac{\varepsilon_\omega}{\varepsilon_\gamma + \varepsilon_\omega} \langle c_\omega \rangle^\omega \tag{4}$$

On the other hand, the time-infinite comportment of the first two spatial moments reveals that two-equation models have a time-asymptotic behavior which can be described in terms of a classical advection/dispersion one-equation model (Eq. (5)) [21,22]. It corresponds to a particular time constrained local non-equilibrium situation for which the tracer does not exhibit anomalous dispersion.

One-equation time-asymptotic non-equilibrium model:

$$(\varepsilon_\gamma + \varepsilon_\omega) \partial_t \langle c \rangle^{\gamma\omega} + \mathbf{V} \cdot \nabla \langle c \rangle^{\gamma\omega} = \nabla \cdot \left\{ \mathbf{D}^{\infty} \cdot \nabla \langle c \rangle^{\gamma\omega} \right\} \tag{5}$$

Apart from this two-equation model and its two particular behaviors, a one-equation non-equilibrium theory (Eq. (6)), based on a very distinct background, is available in [1] for mass transport and in [2] for heat transfer.

One-equation special decomposition non-equilibrium model:

$$(\varepsilon_\gamma + \varepsilon_\omega) \partial_t \langle c \rangle^{\gamma\omega} + \mathbf{V} \cdot \nabla \langle c \rangle^{\gamma\omega} = \nabla \cdot \left\{ \mathbf{D}^{*} \cdot \nabla \langle c \rangle^{\gamma\omega} \right\} \tag{6}$$

The method used for the development of this model differs from the volume averaging with closure theory and finds its essence in a peculiar perturbation decomposition. This one-equation non-equilibrium model can also be obtained using the homogenization theory and this has been devised in [2]. Numerical simulations in [1] suggest that both one-equation local non-equilibrium models (Eqs. (5) and (6)) might be one and the same. However, it is not straightforward from the expression of the dispersion tensors $\mathbf{D}^{\infty}$ and $\mathbf{D}^{*}$. The main goal of this paper is to advance a formal proof for this equivalence (Fig. 2). As an aside, it is interesting to emphasize that very few effort has been dedicated to establishing connections between the various upscaling techniques. Noticeable exceptions are a comparison of ensemble averaging and volume averaging [23], a comparison of the moment matching technique and the homogenization theory [24], a comparison of the homogenization theory and the volume averaging theory [25] and an equivalence between the continuous time random walk technique and the volume averaging theory [26].

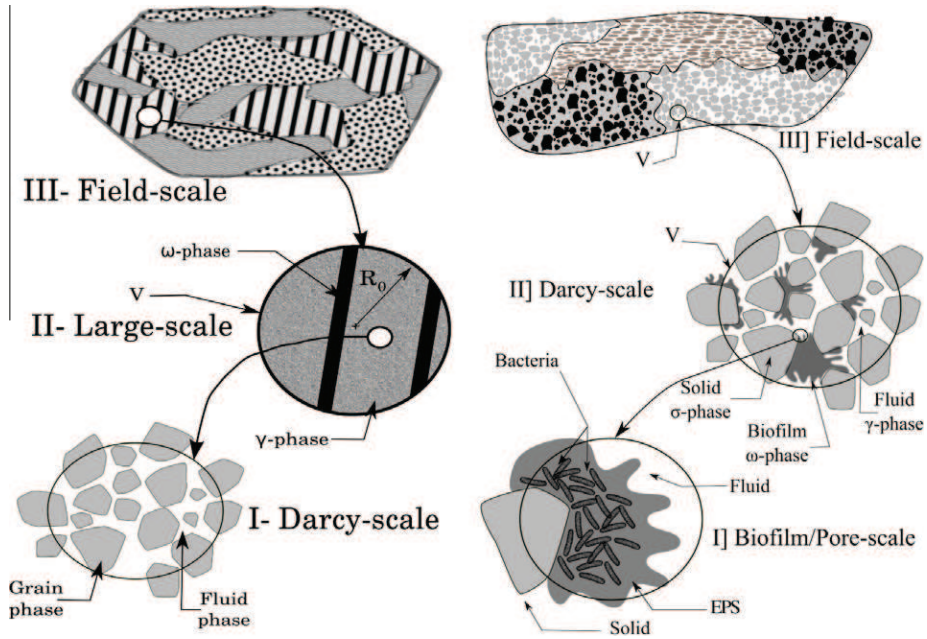

Fig. 1. Hierarchy of the different scales for dual-region large-scale averaging (on the left) and dual-phase Darcy-scale averaging (on the right).

Establishing the domains of validity of macroscopic models represents a critical issue for both theoriticians and experimenters. The procedure of upscaling aims to reduce the number of degrees of freedom of a problem by eliminating redundance in the information at the microscopic scale (see in [27]). It must be understood that the quantity of information that must be eliminated depends on the problem itself but also on the tolerance that one has toward the solutions. Hence, constraints are usually expressed in terms of orders of magnitude of dimensionless numbers such as the Péclet number for example. For the dual-region situation, the reader is referred to the discussion in [28] and more specifically to the Fig. 2 which provides a very good description of the domains of validity of the different models in terms of two Péclet numbers and the ratio between the two. In this article, we show that a temporal axis must also be considered and we discuss the effect of the boundary conditions on these domains.

The remainder of this article is organized as follows. First, we describe the quasi-stationary two-equation model, associated to a *two-phase* system (*phase* might be replaced by *region* when working at the Darcy's scale), its time-asymptotic and local mass equilibrium behaviors along with the model obtained through the special perturbation decomposition. Then, we present the strict equivalence between both one-equation local non-equilibrium models. Finally, numerical computations illustrating the performances of the various models on a very simple 2D geometry are shown and the domains of validity of each model are established for this specific problem.

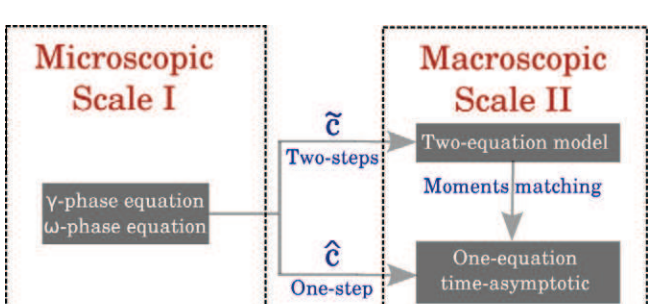

Fig. 2. Schematic representation of both methods.

2. Upscaling

2.1. Microscopic problem

Our study starts with the microscopic description of the medium. The γ-*phase* and the ω-*phase* are both subject to advection and diffusion and the velocity field is supposed to be known pointwise in the whole system. Mass balanced equations for this two-phase system take the form

$$\partial_t c_i + \mathbf{v}_i \cdot \nabla c_i = \nabla \cdot \{\mathbf{D}_i \cdot \nabla c_i\} \tag{7}$$

Here, i represents whether γ or ω. c_i (respectively $\mathbf{v}_i$ and $\mathbf{D}_i$) is the concentration (respectively velocity field and effective dispersion tensor) in the *i-phase*. Associated boundary conditions under consideration are

$$\text{B.C.1}: \quad c_\gamma = c_\omega \quad \text{on } A_{\gamma\omega} \tag{8a}$$

$$\text{B.C.2}: \quad \mathbf{n}_{\gamma\omega} \cdot \mathbf{j}_{c_\gamma} = \mathbf{n}_{\gamma\omega} \cdot \mathbf{j}_{c_\omega} \quad \text{on } A_{\gamma\omega} \tag{8b}$$

$$\text{B.C.3}: \quad \mathbf{n}_{i\sigma} \cdot \mathbf{j}_{c_i} = 0 \quad \text{on } A_{i\sigma} \tag{8c}$$

where $\mathbf{j}_{c_i}$ is the interfacial flux vector, that is $\mathbf{j}_{c_i} = \mathbf{v}_i c_i - \mathbf{D_i} \cdot \nabla c_i$. $\mathbf{n}_{\gamma\omega}$ is the normal vector to the boundary $A_{\gamma\omega}$ between both phases, pointing from γ to ω. The B.C.3, between the phases γ, ω and the grains σ, appears only when upscaling from the pore-scale to the Darcy-scale. For the sake of simplicity and because its derivation is straightforward, this boundary is not considered in the rest of the paper.

2.2. Volume averaging with closure

In this section, we present the main concepts of the volume averaging with closure theory. However, some details of the mathematics, extensively discussed in other articles of the literature, are not given. Our goal is not to cloud important issues with unnecessary equations. A precise literature review allows the unfamiliar and interested reader to easily reconstitute the puzzle.

We study hierarchical porous media, that is, the hypothesis of separation of length scales is assumed to be valid

$$l_\gamma, l_\omega \ll R_0 \ll L \tag{9}$$

where l_i is a characteristic length of the *i-phase* processes, R_0 is the radius of a Representative Elementary Volume (REV) and L is a characteristic length of the *field-scale*. We name V the total volume of a REV and V_i the volume of the *i-phase* within the REV.

During the integration of the microscopic equations, *superficial average* as defined by Eq. (10) appears naturally

$$\langle \Phi_i \rangle = \frac{1}{V}\int_V \Phi_i \, dV \tag{10}$$

When the microscopic concentration is constant throughout the whole phase/region, one usually expects the mean concentration on this phase/region to be equal to the same constant. For this purpose, we define an *intrinsic average* (Eq. (11)) as

$$\langle \Phi_i \rangle^i = \frac{1}{V_i}\int_V \Phi_i \, dV \tag{11}$$

Both measures are linked by

$$\langle \Phi_i \rangle = \varepsilon_i \langle \Phi_i \rangle^i \tag{12a}$$

$$\varepsilon_i = \frac{V_i}{V} \tag{12b}$$

where the volume fraction ε_i is taken to be constant, for the sake of simplicity. We also introduce a weighted averaged concentration (Eq. (13)) which extends the principle of intrinsic average to both phases/regions and is used to describe the transport of the total mass using one-equation models.

$$\langle c \rangle^{\gamma\omega} = \frac{\varepsilon_\gamma}{\varepsilon_\gamma + \varepsilon_\omega}\langle c_\gamma \rangle^\gamma + \frac{\varepsilon_\omega}{\varepsilon_\gamma + \varepsilon_\omega}\langle c_\omega \rangle^\omega \tag{13}$$

The boundary-value problem (Eqs. (7) and (8)) is upscaled using volume averaging with closure as described in [13]. In essence, this method is based on averaging of the spatial operators and on a decomposition of the pointwise concentration into an average plus a fluctuation. Eq. (7) is integrated on a REV, then the average of the derivatives are expressed in terms of derivatives of the averaged plus integrals on the boundaries through the *spatial averaging theorem* [29,30] and the *general transport theorem* [31]. One usually has to face the problem of finding a connection between perturbations and averaged quantities through the resolution of what are called closure problems. The various processes which lead to the classical forms are not detailed because full derivation can be found elsewhere [1,32].

2.2.1. Two-equation model

The classical formulation consists in closing the problem on Gray's perturbations, that is, to decompose concentrations as

$$c_i = \langle c_i \rangle^i + \tilde{c}_i \tag{14}$$

Eq. (14) means that the pointwise concentration is decomposed separately for both physical phases/regions as an intrinsic average on the phase/region plus a fluctuation. The objective is to split the microscopic concentration into quantities varying at different scales. Then, the problem is closed by imposing [22,Eq. (48)] (in which η is used instead of γ)

$$\tilde{c}_i = \sum_{k=\gamma,\omega} \mathbf{b}_{ik} \cdot \nabla \langle c_k \rangle^k - r_i\left(\langle c_\gamma \rangle^\gamma - \langle c_\omega \rangle^\omega\right) \tag{15}$$

This source term decomposition, based on the superposition principle of linear operators, authorises to fully uncouple the boundary-value problems on $\mathbf{b}_{ik}$ and r_i from the macroscopic quantities. It leads, under a quasi-stationary hypothesis on the problem for $\tilde{c}_i$, to the following two-equation model with an exchange term α^{**} between both phases [22] Eqs (58) and (60) (in which η is used instead of γ)

$$\begin{aligned}\varepsilon_i \partial_t \langle c_i \rangle^i &+ \mathbf{V}_{\mathrm{li}}^{**} \cdot \nabla \langle c_i \rangle^i + \mathbf{V}_{ij}^{**} \cdot \nabla \langle c_j \rangle^j \\ &= \nabla \cdot \left\{ \mathbf{D}_{\mathrm{li}}^{**} \cdot \nabla \langle c_i \rangle^i \right\} + \nabla \cdot \left\{ \mathbf{D}_{ij}^{**} \cdot \nabla \langle c_j \rangle^j \right\} - \alpha^{**}\left\{ \langle c_i \rangle^i - \langle c_j \rangle^j \right\}\end{aligned} \tag{16}$$

We do not specify the entire set of effective parameters of the two-equation problem because they can be found in [22, Eqs. (59) and (61)] (in which η is used instead of γ). Meanwhile, it is important to keep in mind that the exchange coefficient α^{**} is only a part of the total interfacial flux, the rest being included in the velocities V_{ij}, and can be expressed as [22, Eq. (54)] (in which η is used instead of γ)

$$\alpha^{**} = -\frac{1}{V}\int_{A_{\gamma\omega}} \mathbf{n}_{\gamma\omega} \cdot \left(\mathbf{v}_\gamma r_\gamma - \mathbf{D}_\gamma \cdot \nabla r_\gamma\right) dA \tag{17}$$

It must be understood that this first order expansion (Eq. (15)) loses some features of the real concentration fields. This created some confusion in the literature about the value of the mass exchange coefficient (see [33] for a discussion).

One-equation local mass equilibrium:

The local mass equilibrium situation corresponds to

$$\langle c_\gamma \rangle^\gamma \cong \langle c_\omega \rangle^\omega \cong \langle c \rangle^{\gamma\omega} \tag{18}$$

In other words, this means that the concentration gradients within the phases/regions are sufficiently small to extend the thermodynamic equilibrium at the interface to the bulk phases/regions. This represents a very particular physical situation for which the total mass within the medium can be described by a single weighted concentration $\langle c \rangle^{\gamma\omega}$, that is, by a one-equation model such as Eq. (19). The associated constraints have been extensively discussed and can be found in [13,34–36]. These are usually expressed in terms of orders of magnitude of dimensionless numbers. In this situation, a reasonable approximation [13] of the two-equation model is [1, Eq. (20)] (in which η is used instead of γ)

$$(\varepsilon_\gamma + \varepsilon_\omega)\partial_t \langle c \rangle^{\gamma\omega} + \mathbf{V} \cdot \nabla \langle c \rangle^{\gamma\omega} = \nabla \cdot \left\{ \mathbf{D}^{equ} \cdot \nabla \langle c \rangle^{\gamma\omega} \right\} \tag{19}$$

It can be obtained by summing Eqs. (1) and (2) and, therefore, the local mass equilibrium dispersion tensor can be written [1, Eq. (22)] (in which η is used instead of γ)

$$\mathbf{D}^{equ} = \sum_{i,j=\gamma \text{ or } \omega} \mathbf{D}_{ij}^{**} = \sum_{k=\gamma,\omega} \varepsilon_k \langle \mathbf{D}_k \cdot (\mathbf{I} + \nabla \mathbf{B}_k) - \tilde{\mathbf{v}}_k \mathbf{B}_k \rangle^k \tag{20}$$

The effective velocity takes the very simple form [1, Eq. (23)] (in which η is used instead of γ)

$$\mathbf{V} = \varepsilon_\gamma \langle \mathbf{v}_\gamma \rangle^\gamma + \varepsilon_\omega \langle \mathbf{v}_\omega \rangle^\omega \tag{21}$$

One-equation time-asymptotic non-equilibrium model:

Matching the first two spatial moments [21] (in which α, β is used instead of γ, ω), one is able to find that the two-equation model has a one-equation time-asymptotic behavior which can be written [22, Eq. (67)] (in which η is used instead of γ)

$$(\varepsilon_\gamma + \varepsilon_\omega)\partial_t \langle c \rangle^{\gamma\omega} + \mathbf{V} \cdot \nabla \langle c \rangle^{\gamma\omega} = \nabla \cdot \left\{ \mathbf{D}^\infty \cdot \nabla \langle c \rangle^{\gamma\omega} \right\} \tag{22}$$

In essence, this means that the description of the mass transport at long times can be undertaken using an advection–dispersion type equation, that is, the behavior of higher order moments can be neglected. It is not clear in the literature what are the physical and temporal constraints which allow such an approximation. This is beyond the scope of this study to provide such an analysis but this aspect of the problem will be the subject of further investigation.

The dispersion tensor (Eq. (50)) can be written [21, Eqs. (97)–(99)]

$$\mathbf{D}^{\infty} = \sum_{i,j=\gamma \text{ or } \omega} \mathbf{D}_{ij}^{**} + \frac{1}{\alpha^{**}}\left(\mathbf{U}^{*} + \mathbf{d}_{\omega}^{**} - \mathbf{d}_{\gamma}^{**}\right)(\mathbf{U}^{*} - \boldsymbol{\beta}^{*})$$
$$= \mathbf{D}^{equ} + \frac{1}{\alpha^{**}}\left(\mathbf{U}^{*} + \mathbf{d}_{\omega}^{**} - \mathbf{d}_{\gamma}^{**}\right)(\mathbf{U}^{*} - \boldsymbol{\beta}^{*}) \tag{23}$$

Both parts of this expression have very distinct physical meaning. $\sum_{i,j=\gamma \text{ or } \omega}\mathbf{D}_{ij}^{**}$ represents the sum of the dispersion terms, which strictly speaking, corresponds to local mass equilibrium dispersion, and is rather similar to the single phase situation. However, the second part stands for the multiphase aspects. It expresses the contrast between the γ-*phase* and the ω-*phase*. It tends toward *0* when the exchange coefficient α^{**} tends toward infinity and is mainly driven by the square of

$$\mathbf{U}^{*} = \varepsilon_{\gamma}\varepsilon_{\omega}\frac{\langle \mathbf{v}_{\gamma}\rangle^{\gamma} - \langle \mathbf{v}_{\omega}\rangle^{\omega}}{\varepsilon_{\gamma} + \varepsilon_{\omega}} \tag{24}$$

It also contains

$$\boldsymbol{\beta}^{*} = -\frac{1}{V}\int_{A_{\gamma\omega}} \mathbf{n}_{\gamma\omega}\cdot \mathbf{j}_{\mathbf{B}_{\gamma}}\, dA \tag{25a}$$
$$\mathbf{d}_{\omega}^{**} - \mathbf{d}_{\gamma}^{**} = \sum_{k=\gamma,\omega}\varepsilon_{k}\langle \mathbf{D}_{k}\cdot\nabla r_{k} - \tilde{\mathbf{v}}_{k} r_{k}\rangle^{k} \tag{25b}$$

This asymptotic behavior was proved directly from the lower-scale equation in [37] for stratified systems, and used extensively in [19] which introduced the word Taylor's dispersion, for that particular case, because of the square dependence of the dispersion coefficient with the velocity difference.

Notice that there are usually six closure (or mapping) variables associated to the two-equation model, that is $\mathbf{b}_{\gamma\gamma}$, $\mathbf{b}_{\gamma\omega}$, $\mathbf{b}_{\omega\gamma}$, $\mathbf{b}_{\omega\omega}$, r_{γ}, r_{ω}. In the expression of the dispersion (Eq. (23)) only four closure variables remain, namely r_{γ}, r_{ω} and $\mathbf{B}_{\gamma}$, $\mathbf{B}_{\omega}$. They are simply related to those of the two-equation model by

$$\mathbf{B}_{\gamma} = \mathbf{b}_{\gamma\gamma} + \mathbf{b}_{\gamma\omega} \tag{26a}$$
$$\mathbf{B}_{\omega} = \mathbf{b}_{\omega\gamma} + \mathbf{b}_{\omega\omega} \tag{26b}$$

Closure problems:

The set of effective parameters previously introduced can be computed through the resolution of the two following closure problems. They can be straightforwardly derived from [22, Eqs. (49)–(56)] (in which η is used instead of γ).

$$\mathbf{v}_{\gamma}\cdot\nabla r_{\gamma} = \nabla\cdot\left\{\mathbf{D}_{\gamma}\cdot\nabla r_{\gamma}\right\} - \varepsilon_{\gamma}^{-1}\alpha^{**} \tag{27a}$$
$$\text{B.C.1}: \quad r_{\gamma} = r_{\omega} \tag{27b}$$
$$\text{B.C.2}: \quad -\mathbf{n}_{\gamma\omega}\cdot\left(\mathbf{j}_{r_{\gamma}} - \mathbf{j}_{r_{\omega}}\right) = 0 \tag{27c}$$
$$\mathbf{v}_{\omega}\cdot\nabla r_{\omega} = \nabla\cdot\{\mathbf{D}_{\omega}\cdot\nabla r_{\omega}\} + \varepsilon_{\omega}^{-1}\alpha^{**} \tag{27d}$$

$$\mathbf{v}_{\gamma}\cdot\nabla\mathbf{B}_{\gamma} = \nabla\cdot\left\{\mathbf{D}_{\gamma}\cdot\nabla\mathbf{B}_{\gamma}\right\} - \tilde{\mathbf{v}}_{\gamma} - \varepsilon_{\gamma}^{-1}\boldsymbol{\beta}^{*} \tag{28a}$$
$$\text{B.C.1}: \quad \mathbf{B}_{\gamma} = \mathbf{B}_{\omega} \tag{28b}$$
$$\text{B.C.2}: \quad -\mathbf{n}_{\gamma\omega}\cdot\left(\mathbf{j}_{\mathbf{B}_{\gamma}} - \mathbf{j}_{\mathbf{B}_{\omega}}\right) = -\mathbf{n}_{\gamma\omega}\cdot\left(\mathbf{D}_{\omega} - \mathbf{D}_{\gamma}\right) \tag{28c}$$
$$\mathbf{v}_{\omega}\cdot\nabla\mathbf{B}_{\omega} = \nabla\cdot\{\mathbf{D}_{\omega}\cdot\nabla\mathbf{B}_{\omega}\} - \tilde{\mathbf{v}}_{\omega} + \varepsilon_{\omega}^{-1}\boldsymbol{\beta}^{*} \tag{28d}$$

2.3. Special perturbation decomposition

A different way to obtain one-equation local non-equilibrium models consists in decomposing concentrations as follows:

$$c_{i} = \langle c\rangle^{\gamma\omega} + \hat{c}_{i} \tag{29}$$

In this case, the fluctuation is defined in relation to the weighted average on both phases/regions. The problem is closed using [1, Eq. (52)] (in which η is used instead of γ), [2, Eqs. (42) and (43)], for heat transfer (in which β, σ is used instead of γ, ω)

$$\hat{c}_{i} = \mathbf{b}_{i}\cdot\nabla\langle c\rangle^{\gamma\omega} \tag{30}$$

It has been proposed in [1] for the large-scale averaging problem and applied in [38] for a reactive case (linear kinetics). This decomposition may be very efficient since it allows to directly develop a macroscopic one-equation model, to reduce the number of closure parameters and it is also useful for upscaling various class of problems such as reactive ones. The counterpart is that the assumptions behind the first order closure and the quasi-stationarity of the fluctuations problems are stronger in this case because (1) the closure recovers less characteristic times than the $\tilde{c}$ decomposition and (2) the norm of the $\hat{c}_{i}$ perturbation is larger than the norm of $\tilde{c}_{i}$. The macroscopic mass balanced equation takes the form [1, Eq. (56)] (in which η is used instead of γ)

$$\left(\varepsilon_{\gamma} + \varepsilon_{\omega}\right)\partial_{t}\langle c\rangle^{\gamma\omega} + \mathbf{V}\cdot\nabla\langle c\rangle^{\gamma\omega} = \nabla\cdot\left\{\mathbf{D}^{*}\cdot\nabla\langle c\rangle^{\gamma\omega}\right\} \tag{31}$$

The $\hat{c}_{i}$ perturbation decomposition leads to the following expression of dispersion, see in [1, Eq. (57)] (in which η is used instead of γ) and [38].

$$\mathbf{D}^{*} = \sum_{k=\gamma,\omega}\varepsilon_{k}\left[\mathbf{D}_{k}\cdot\left(\mathbf{I} + \langle\nabla\mathbf{b}_{k}\rangle^{k}\right) - \langle\mathbf{v}_{k}\mathbf{b}_{k}\rangle^{k}\right] \tag{32}$$

Closure problem:

The determination of effective parameters requires the calculation of a single problem which can be found in [1, Eqs. (53)– (55)] (in which η is used instead of γ) and in [38].

$$\mathbf{v}_{\gamma}\cdot\nabla\mathbf{b}_{\gamma} = \nabla\cdot\left\{\mathbf{D}_{\gamma}\cdot\nabla\mathbf{b}_{\gamma}\right\} - \tilde{\mathbf{v}}_{\gamma} - \varepsilon_{\gamma}^{-1}\boldsymbol{U}^{*} \tag{33a}$$
$$\text{B.C.1}: \quad \mathbf{b}_{\gamma} = \mathbf{b}_{\omega} \tag{33b}$$
$$\text{B.C.2}: \quad -\mathbf{n}_{\gamma\omega}\cdot\left(\mathbf{j}_{\mathbf{b}_{\gamma}} - \mathbf{j}_{\mathbf{b}_{\omega}}\right) = -\mathbf{n}_{\gamma\omega}\cdot\left(\mathbf{D}_{\omega} - \mathbf{D}_{\gamma}\right) \tag{33c}$$
$$\mathbf{v}_{\omega}\cdot\nabla\mathbf{b}_{\omega} = \nabla\cdot\{\mathbf{D}_{\omega}\cdot\nabla\mathbf{b}_{\omega}\} - \tilde{\mathbf{v}}_{\omega} + \varepsilon_{\omega}^{-1}\boldsymbol{U}^{*} \tag{33d}$$

3. Formal equivalence

The goal of this part is to obtain a formal proof of the equivalence between Eqs. (22) and (31), that is, to prove $\mathbf{D}^{*} = \mathbf{D}^{\infty}$.

3.1. Mathematical development

At this point, the mapping variables r_{γ}, r_{ω}, $\mathbf{B}_{\gamma}$, $\mathbf{B}_{\omega}$ and $\mathbf{b}_{\gamma}$, $\mathbf{b}_{\omega}$ are solutions of different boundary-value problems (Eqs. (27), (28) and (33)). In order to find a relationship between these closure variables, we introduce the following source terms decomposition based on the superposition principle for linear operators

$$\mathbf{B}_{i} = \mathbf{B}_{\mathrm{I}i} + B_{\mathrm{II}i}\boldsymbol{\beta}^{*} \tag{34a}$$
$$\mathbf{b}_{i} = \mathbf{b}_{\mathrm{I}i} + b_{\mathrm{II}i}\mathbf{U}^{*} \tag{34b}$$
$$r_{i} = r_{\mathrm{II}i}\alpha^{**} \tag{34c}$$

As a consequence of the previous decomposition, Eqs. (27), (28) and (33) reduce to only two boundary-value problems. $\mathbf{B}_{\mathrm{I}i}$ and $\mathbf{b}_{\mathrm{I}i}$ are solutions of the following closure problem type I

$$\mathbf{v}_{\gamma}\cdot\nabla\boldsymbol{\Phi}_{\mathrm{I}\gamma} = \nabla\cdot\left\{\mathbf{D}_{\gamma}\cdot\nabla\boldsymbol{\Phi}_{\mathrm{I}\gamma}\right\} - \tilde{\mathbf{v}}_{\gamma} \tag{35a}$$
$$\text{B.C.1}: \quad \boldsymbol{\Phi}_{\mathrm{I}\gamma} = \boldsymbol{\Phi}_{\mathrm{I}\omega} \tag{35b}$$
$$\text{B.C.2}: \quad -\mathbf{n}_{\gamma\omega}\cdot\left(\mathbf{j}_{\boldsymbol{\Phi}_{\mathrm{I}\gamma}} - \mathbf{j}_{\boldsymbol{\Phi}_{\mathrm{I}\omega}}\right) = -\mathbf{n}_{\gamma\omega}\cdot\left(\mathbf{D}_{\omega} - \mathbf{D}_{\gamma}\right) \tag{35c}$$
$$\mathbf{v}_{\omega}\cdot\nabla\boldsymbol{\Phi}_{\mathrm{I}\omega} = \nabla\cdot\{\mathbf{D}_{\omega}\cdot\nabla\boldsymbol{\Phi}_{\mathrm{I}\omega}\} - \tilde{\mathbf{v}}_{\omega} \tag{35d}$$

Table 1
Equivalence of the approximations associated to the volume averaging theory and to the moments matching technique.

Approximation of	Moments matching technique	Volume averaging theory
Convolutions in space	Spatial moments matching up to the second order	First order closure
Convolutions in time	Time-infinite behavior of the spatial moments	Quasi-stationarity of the closure problems

Unicity of the solutions is provided by the following conditions

$$\varepsilon_\gamma \langle \mathbf{B}_{\mathrm{I}\gamma} \rangle^\gamma + \varepsilon_\omega \langle \mathbf{B}_{\mathrm{I}\omega} \rangle^\omega = \mathbf{0} \tag{36a}$$

$$\varepsilon_\gamma \langle \mathbf{b}_{\mathrm{I}\gamma} \rangle^\gamma + \varepsilon_\omega \langle \mathbf{b}_{\mathrm{I}\omega} \rangle^\omega = \mathbf{0} \tag{36b}$$

$B_{\mathrm{II}i}$, $b_{\mathrm{II}i}$ and $r_{\mathrm{II}i}$ are solutions of the following closure problem Type II

$$\mathbf{v}_\gamma \cdot \nabla \Phi_{\mathrm{II}\gamma} = \nabla \cdot \left\{ \mathbf{D}_\gamma \cdot \nabla \Phi_{\mathrm{II}\gamma} \right\} - \varepsilon_\gamma^{-1} \tag{37a}$$

$$\text{B.C.1}: \quad \Phi_{\mathrm{II}\gamma} = \Phi_{\mathrm{II}\omega} \tag{37b}$$

$$\text{B.C.2}: \quad -\mathbf{n}_{\gamma\omega} \cdot \left(\mathbf{j}_{\Phi_{\mathrm{II}\gamma}} - \mathbf{j}_{\Phi_{\mathrm{II}\omega}} \right) = 0 \tag{37c}$$

$$\mathbf{v}_\omega \cdot \nabla \Phi_{\mathrm{II}\omega} = \nabla \cdot \{ \mathbf{D}_\omega \cdot \nabla \Phi_{\mathrm{II}\omega} \} + \varepsilon_\omega^{-1} \tag{37d}$$

Unicity of the solutions is provided by the following conditions

$$\varepsilon_\gamma \langle B_{\mathrm{II}\gamma} \rangle^\gamma + \varepsilon_\omega \langle B_{\mathrm{II}\omega} \rangle^\omega = 0 \tag{38a}$$

$$\varepsilon_\gamma \langle b_{\mathrm{II}\gamma} \rangle^\gamma + \varepsilon_\omega \langle b_{\mathrm{II}\omega} \rangle^\omega = 0 \tag{38b}$$

$$\langle r_{\mathrm{II}\omega} \rangle^\omega = \frac{1}{\alpha^{**}}; \quad \langle r_{\mathrm{II}\gamma} \rangle^\gamma = 0 \tag{38c}$$

$\mathbf{b}_{\mathrm{I}i}$ and $\mathbf{B}_{\mathrm{I}i}$ are solutions of the same problem and satisfy the same unicity equation. Hence, we have

$$\mathbf{b}_{\mathrm{I}i} = \mathbf{B}_{\mathrm{I}i} \tag{39}$$

which implies

$$\mathbf{b}_i = \mathbf{B}_i - B_{\mathrm{II}i} \boldsymbol{\beta}^* + b_{\mathrm{II}i} \mathbf{U}^* \tag{40}$$

It is also important to notice that $b_{\mathrm{II}i}$ and $B_{\mathrm{II}i}$ are solution of the same problem Type II and satisfy the same unicity equations so that we have

$$\mathbf{b}_i = \mathbf{B}_i + b_{\mathrm{II}i} (\mathbf{U}^* - \boldsymbol{\beta}^*) \tag{41}$$

Finally $b_{\mathrm{II}i}$ and $r_{\mathrm{II}i}$ are solution of the same problem but do not satisfy the same unicity equations so that they only differ by a constant. After some simple algebra, we obtain

$$\mathbf{b}_i = \mathbf{B}_i + \frac{1}{\alpha^{**}} \left(r_i - \frac{\varepsilon_\omega}{(\varepsilon_\gamma + \varepsilon_\omega)} \right) (\mathbf{U}^* - \boldsymbol{\beta}^*) \tag{42}$$

3.2. Conclusion and discussion

Injecting this expression of $\mathbf{b}_i$, i.e. Eq. (42), in Eq. (32) straightforwardly leads to

$$\mathbf{D}^* = \mathbf{D}^\infty \tag{43}$$

One may realize that the physics underlying the time-asymptotic hypothesis in one-phase or two-phase systems have very different backgrounds. In the single-phase configuration, the equality of the dispersion tensors between the volume averaging theory as devised by Whitaker [13] and the moments matching technique as devised by Brenner [39] is straightforward. In this single-phase case, the problem is not homogenizable at very short times, that is, one needs to consider only long times to avoid the convolutions. This limitation corresponds to the time needed for a particle to visit the entire microscopic domain. In a dual-phase situation, this assumption of the single-phase case is reminiscent to the quasi-stationary hypothesis on the standard perturbations, although not exactly similar because of the contrast of properties and of the exchange between both phases. The time-asymptotic behavior of the two-equation model corresponds to a macroscopic relaxation of the two-equation boundary-value problem, that is, a relaxation of the first two spatial moments or of the nonstandard perturbation. This represents a very different approximation.

The result expressed by Eq. (43) provides a direct equivalence between the moments matching method and a special volume averaging theory based on a different decomposition technique. This conclusion has various consequences.

- Two-equation models provide a solid basis for exploring physical aspects of the dispersion problem.
- Going back to the discussion about the choice of the proper mass transfer coefficient (see [33,26]) the results obtained in this paper show that the other proposed values would lead to an incorrect asymptotic dispersion equation, even if they can work better at some limited stages of the transient evolution.
- We use the moments matching technique on an already homogenized set of equations, that is, we do not start at the microscopic scale as proposed in [39]. Although it has not been devised yet, we believe that the two-equation model can be obtained using the method in [39] and the equivalence developed in this article strongly reinforces the relationship between the volume averaging theory and the moments matching techniques.
- This equality (Eq. (43)) also allows to see a similar problem from two different viewpoints Table 1. The long time limit is traduced, in the $\hat{c}$ decomposition, as a quasi-stationary closure problem and this is a new interesting way of seeing the time-asymptotic hypothesis in the multiphase configuration. Moreover, Eq. (43) shows that a very strong relationship exists between the closure on $\hat{c}$ and the moments matching method limited to the second order, as applied in [21,22].

4. A simple example: a 2D medium

In this part, we are interested in computing the previous models on a simple 2D geometry (Fig. 3) in order to catch the main characteristics of the problem. We show that even for an input signal introducing many characteristic times, the time-asymptotic model may give a rather good approximation at short times and gains in precision as the time tends toward infinity.

The γ-*phase* is convective and diffusive whereas the ω-*phase* is only diffusive (called mobile–immobile situation). One example of such a system could be the study of a tracer transport between two plates colonized by biofilms (aggregations of micro-organisms coated in protective extra-cellular substances). The closure problems type I and type II (Fig. 4) presented in the next section are solved using the Comsol™ multiphysics package. Notice that

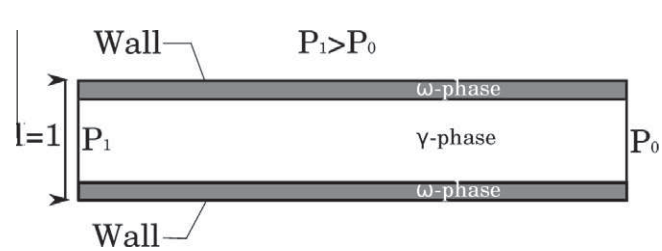

Fig. 3. Schematic description of the 2D system.

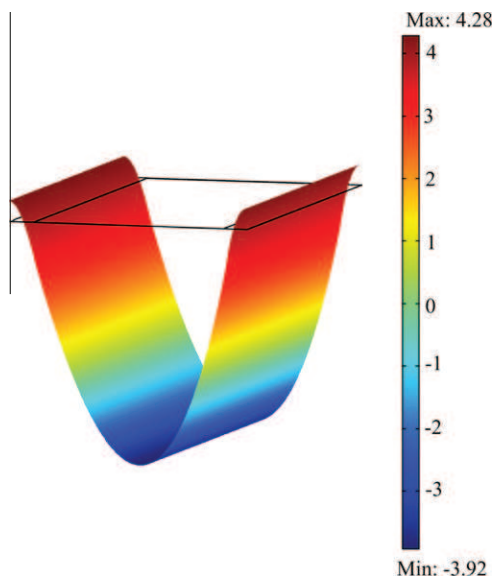

Fig. 4. Norm of the b_i field for $Pe = 200$.

because of the very particular geometry and because we impose periodic boundary conditions, the closure field is 1D. We also fully solve the balanced momentum equations so that we do not consider any upscaling of momentum equations. The closure problems only depends upon a Péclet number defined as

$$Pe = \frac{\langle v_\gamma \rangle^\gamma L}{D_\gamma} \tag{44}$$

where we choose

$$L = 1 \tag{45a}$$

$$\frac{D_\omega}{D\gamma} = 0.8 \tag{45b}$$

$$\varepsilon_\omega = 0.2 \tag{45c}$$

The dimensionless time is defined by

$$t' = \frac{\langle v_\gamma \rangle t}{L} \tag{46}$$

and the concentration is normalized to the amplitude of the input concentration.

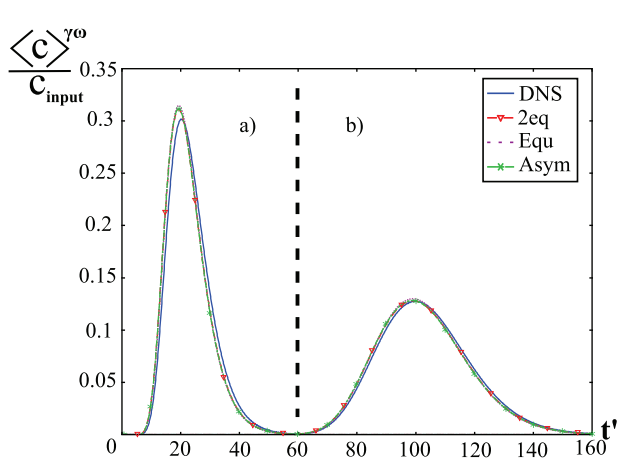

Fig. 5. Breakthrough curves for $Pe = 2$ after (a) $10L$ and (b) $50L$ for a square input of width $\delta t' = 5$ starting at $t' = 0$. The solid line corresponds to the DNS, the dotted line to the local mass equilibrium model, the dashed line with triangles to the two-equation model and the dashed-dotted line with stars to the time-asymptotic model.

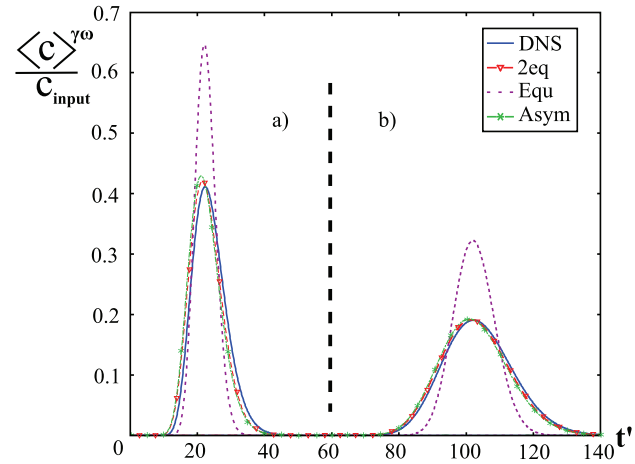

Fig. 6. Breakthrough curves for $Pe = 20$ after (a) $10L$ and (b) $50L$ for a square input of width $\delta t' = 5$ starting at $t' = 0$. The solid line corresponds to the DNS, the dotted line to the local mass equilibrium model, the dashed line with triangles to the two-equation model and the dashed-dotted line with stars to the time-asymptotic model.

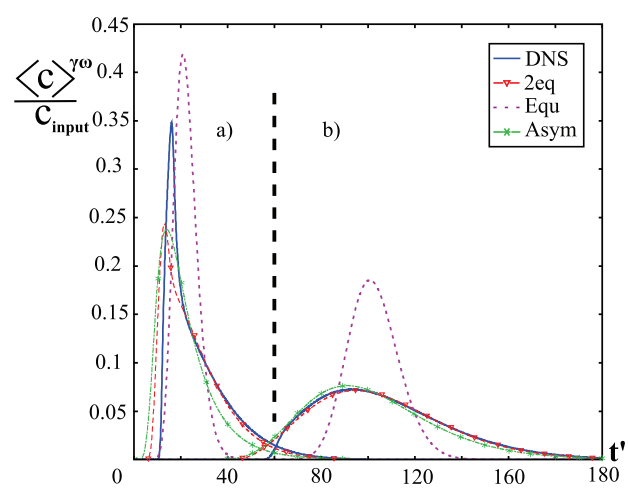

Fig. 7. Breakthrough curves for $Pe = 200$ after (a) $10L$ and (b) $50L$ for a square input of width $\delta t' = 5$ starting at $t' = 0$. The solid line corresponds to the DNS, the dotted line to the local mass equilibrium model, the dashed line with triangles to the two-equation model and the dashed-dotted line with stars to the time-asymptotic model.

On the one hand, we solve the entire 2D microscopic problem on a total length of $60L$ (called DNS for Direct Numerical Simulation) for a square input for different Péclet numbers. On the other hand, we solve the 1D upscaled local equilibrium, non-equilibrium and two-equation models on a total length of $60L$ (Fig. 5–7). Then, we observe breakthrough curves at $10L$ and $50L$ for Péclet numbers of 2, 20 and 200.

In Fig. 5, we see that the three homogenized models provide a very good approximation of the transport problem. At low Péclet, time and space non-locality tend to disappear because time and length scales are separated by several orders of magnitude. Meanwhile, some very little discrepancy still remains at the peak of the signal at $10L$. At the very beginning of the system, the time-width of the signal propagating is of the same order of magnitude as the characteristic time for the relaxation of the effective parameters. When the signal spreads, the non-locality disappears and at $50L$ all the signals are in good agreement. The propagation is even slow enough for the local mass equilibrium assumption to be well-founded, that is, the exchange coefficient is big enough for the

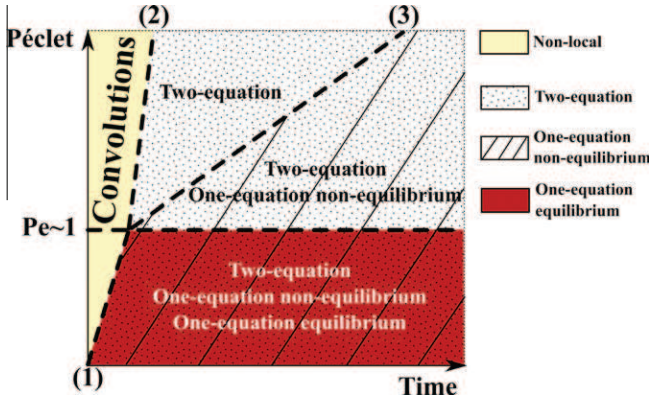

Fig. 8. Domains of validity of the different models as a function of the Péclet number and of the time for a square input signal.

multiphase contrast term in the expression of the time-asymptotic dispersion (Eq. (23)) to be insignificant.

When the Péclet number reaches values around 20, the local mass equilibrium assumption starts to become inappropriate. Fig. 6 shows that the local mass equilibrium model gives a poor approximation of the signal whereas both non-equilibrium models are still in good agreement. The fact that the peaks for these two models arise earlier than the one of the DNS is again characteristic of non-locality. Memory functions or fully non-local theories (such as *n*-equations models) should be considered in this case.

For Péclet numbers around 200, Fig. 7, the local mass equilibrium model is completely inaccurate. The two-equation model provides the best approximation because it captures more characteristic times than the time-asymptotic one. Except for non-locality (especially at 10*L*), it recovers the shape of the signal. However, even for a square input signal and high Péclet numbers, the time-asymptotic model is still rather accurate. As the signal spreads, all the non-equilibrium models tend toward the correct solution and this means that domains of validity need a time dimension. Results suggest that the one-equation local non-equilibrium model might represent, in cases such as intermediate Péclet numbers, macroscopic stationarity or asymptotic regimes, a good compromise, in terms of computational demand, between the two-equation and the local mass equilibrium models. The importance of non-locality is also emphasized and becomes particularly obvious in the high Péclet number situation.

On the basis of these results, domains of validity can be determined for a square input signal identical in both phases Fig. 8. When the Péclet number is below or approximately unity, the local mass equilibrium condition is verified except at very short times where fully non-local theories or *n*-equation models should be considered. Above unity, the situation is more complex as three different regimes are identified. At very short times, the situation can not be described even by the quasi-stationary two-equation model and non-local theories are necessary. At intermediate times, the two-equation model represents the only alternative to convolutions. As the time tends toward infinity and the signal spreads, the one-equation non-equilibrium model can be used to describe the mass transport. The boundaries between these different regimes depend, among others, on the input boundary condition, on the microscopic topology and on the processes. The constraints associated to the boundary (1) and (2), Fig. 8, between the non-local and local zone have been extensively discussed [32,22,20,28,8]. However, little is known on the limitations associated with (3), Fig. 8, and it requires further investigation.

Concerning the influence of the boundary conditions on the domains of validity, it is important to emphasize that two-equation models allow to modify separately the conditions for each phase unlike one-equation models. As a consequence, in situations where the boundary conditions in one-phase are very different from the conditions in the other phase, two-equation models must be considered at the expense of one-equation models. Additionally, two-equation models are likely to provide a better approximation of the transport processes when many modes are excited, that is, for a Dirac input for example.

5. Conclusion

In this work, we provide a comparison of deterministic models used in hydrology and chemical engineering, that is, the quasi-stationary two-equation model (Eqs. (47) and (48)), the one-equation local mass equilibrium (Eq. (49)), time-asymptotic (Eq. (50)) and special decomposition (Eq. (51)) models.

Two-equation model:

$$\varepsilon_\gamma \partial_t \langle c_\gamma \rangle^\gamma + \mathbf{V}^{**}_{\gamma\gamma} \cdot \nabla \langle c_\gamma \rangle^\gamma + \mathbf{V}^{**}_{\gamma\omega} \cdot \nabla \langle c_\omega \rangle^\omega = \nabla \cdot \left\{ \mathbf{D}^{**}_{\gamma\gamma} \cdot \nabla \langle c_\gamma \rangle^\gamma \right\} + \nabla \cdot \left\{ \mathbf{D}^{**}_{\gamma\omega} \cdot \nabla \langle c_\omega \rangle^\omega \right\} - \alpha^{**} \left\{ \langle c_\gamma \rangle^\gamma - \langle c_\omega \rangle^\omega \right\} \tag{47}$$

$$\varepsilon_\omega \partial_t \langle c_\omega \rangle^\omega + \mathbf{V}^{**}_{\omega\gamma} \cdot \nabla \langle c_\gamma \rangle^\gamma + \mathbf{V}^{**}_{\omega\omega} \cdot \nabla \langle c_\omega \rangle^\omega = \nabla \cdot \left\{ \mathbf{D}^{**}_{\omega\gamma} \cdot \nabla \langle c_\gamma \rangle^\gamma \right\} + \nabla \cdot \left\{ \mathbf{D}^{**}_{\omega\omega} \cdot \nabla \langle c_\omega \rangle^\omega \right\} - \alpha^{**} \left\{ \langle c_\omega \rangle^\omega - \langle c_\gamma \rangle^\gamma \right\} \tag{48}$$

One-equation local mass equilibrium model:

$$(\varepsilon_\gamma + \varepsilon_\omega) \partial_t \langle c \rangle^{\gamma\omega} + \mathbf{V} \cdot \nabla \langle c \rangle^{\gamma\omega} = \nabla \cdot \left\{ \mathbf{D}^{equ} \cdot \nabla \langle c \rangle^{\gamma\omega} \right\} \tag{49}$$

One-equation time-asymptotic non-equilibrium model:

$$(\varepsilon_\gamma + \varepsilon_\omega) \partial_t \langle c \rangle^{\gamma\omega} + \mathbf{V} \cdot \nabla \langle c \rangle^{\gamma\omega} = \nabla \cdot \left\{ \mathbf{D}^{\infty} \cdot \nabla \langle c \rangle^{\gamma\omega} \right\} \tag{50}$$

One-equation special decomposition non-equilibrium model:

$$(\varepsilon_\gamma + \varepsilon_\omega) \partial_t \langle c \rangle^{\gamma\omega} + \mathbf{V} \cdot \nabla \langle c \rangle^{\gamma\omega} = \nabla \cdot \left\{ \mathbf{D}^{*} \cdot \nabla \langle c \rangle^{\gamma\omega} \right\} \tag{51}$$

- The fundamental analysis carried out in Section 3 leads to $\mathbf{D}^\infty = \mathbf{D}^*$. It has broad practical implications since these one-equation models, because of their intrinsic simplicity, are widely used by experimenters. In addition, these models were obtained using very distinct techniques, that is, moments matching for the time-asymptotic model and a closure on a peculiar perturbation for the model (Eq. (51)). From a theoretical point of view, equivalence between these two methods shows that (1) two-equation models provide a reliable basis for the study of the dispersion problem, (2) the idea of matching moments up to the second order is similar to the closure on the spatial perturbations and (3) the time-asymptotic limit of the moments corresponds to the quasi-stationarity of the perturbation problem.
- The numerical results obtained for a mobile–immobile problem with different Péclet numbers show that (1) the local mass equilibrium model has a restricted area of validity and must be used very carefully (see discussion in [40]), (2) the one-equation non-equilibrium model produces a reasonable approximation of the transport at long times, even for a square input signal and high Péclet numbers, (3) the two-equation model gives, in all cases, better results and (4) domains of validity representations need a time dimension.

Acknowledgement

Support from CNRS/GdR 2990 is gratefully acknowledged.

References

[1] M. Quintard, F. Cherblanc, S. Whitaker, Dispersion in heterogeneous porous media: one-equation non-equilibrium model, Transport Porous Media 44 (2001) 181–203.

[2] C. Moyne, S. Didierjean, H. Amaral Souto, O. da Silveira, Thermal dispersion in porous media: one-equation model, Int. J. Heat Mass Transfer 43 (2000) 3853–3867.

[3] J. Koch, J. Brady, A non-local description of advection–diffusion with application to dispersion in porous media, J. Fluid Mech. 180 (1987) 387–403.

[4] J. Koch, J. Brady, Anomalous diffusion in heterogeneous porous media, Phys. Fluids 31 (1988) 965–973.

[5] J. Cushman, T. Ginn, Non-local dispersion in porous media with countinuously evolving scales of heterogeneity, Transport Porous Media 13 (1993) 123–138.

[6] C. Moyne, Two-equation model for a diffusive process in porous media using the volume averaging method with unsteady-state closure, Adv. Water Resour. 20 (1997) 63–76.

[7] J. Cushman, T. Ginn, Fractional advection–dispersion equation. a classical mass balance with convolution-fickian flux, Water Resour. Res. 36 (2000) 3763–3766.

[8] J. Chastanet, B. Wood, Mass transfer process in a two-region medium, Water Resour. Res. 44 (2008) W05413, doi:10.1029/2006WR005553.

[9] T. Arbogast, Derivation of the double porosity model of single phase flow via homogenization theory, SIAM J. Appl. Math. 21 (1985) 3087–3098.

[10] T. Arbogast, The double porosity model for single phase flow in naturally fractured reservoirs, in: Numerical Simulation in Oil Recovery, IMA Volumes in Mathematics and its Applications, Springer Verlag, New York, 1988.

[11] J. Lewandowska, A. Szymkiewicz, K. Burzyński, M. Vauclin, Modeling of unsaturated water flow in double-porosity soils by the homogenization approach, Adv. Water Resour. 27 (2004) 283–296.

[12] G. Debenest, M. Quintard, Transport in highly heterogeneous porous media: from direct simulation to macro-scale two-equation models or mixed models, Chem. Product Process Model. 3 (1) (2008) (Article 19).

[13] S. Whitaker, The Method of Volume Averaging, Kluwer, Dordrecht, 1999.

[14] K. Coats, B. Smith, Dead end pore volume and dispersion in porous media, Soc. Petrol. Eng. J. 4 (1964) 73–84.

[15] F. De Smedt, P. Wierenga, Mass transfer in porous media with immobile water, J. Hydrol. 41 (1979) 59–67.

[16] M. Goltz, P. Roberts, Three-dimensional solutions for solute transport in an infinite medium with mobile and immobile zones, Water Resour. Res. 22 (7) (1986) 1139–1148.

[17] M. Brusseau, R. Jessup, P. Rao, Modeling the transport of solutes influenced by multiprocess nonequilibrium, Water Resour. Res. 25 (9) (1989) 1971–1988.

[18] A. Correa, K. Pande, H. Ramey, W. Brigham, Computation and interpretation of miscible displacement performance in heterogeneous porous media, SPE (Society of Petroleum Engineers) Reservoir Eng. 5 (1).

[19] L. Lake, G. Hirasaki, Taylor's dispersion in stratified porous media, SPE J. (1981) 459–468.

[20] F. Cherblanc, A. Ahmadi, M. Quintard, Two-domain description of solute transport in heterogeneous porous media: comparison between theoretical predictions and numerical experiments, Adv. Water Resour. 30 (2007) 1127–1143.

[21] F. Zanotti, R. Carbonell, Development of transport equations for multiphase systems I: general development for two-phase systems, Chem. Eng. Sci. 39 (1984) 263–278.

[22] A. Ahmadi, M. Quintard, S. Whitaker, Transport in chemically and mechanically heterogeneous porous media V: two-equation model for solute transport with adsorption, Adv. Water Resour. 22 (1998) 59–86.

[23] B. Wood, F. Cherblanc, M. Quintard, S. Whitaker, Volume averaging for determining the effective dispersion tensor: closure using periodic unit cells and comparison with ensemble averaging, Water Resour. Res. 39 (2003) 1210.

[24] J. Auriault, P. Adler, Taylor dispersion in porous media: analysis by multiple scale expansions, Adv. Water Resour. 18 (1995) 217–226.

[25] A. Bourgeat, M. Quintard, S. Whitaker, Comparison between homogenization theory and volume averaging method with closure problem, Comptes Rendus de l'Académie des Sciences, Série 2 306 (1988) 463–466.

[26] B. Noetinger, T. Estebenet, M. Quintard, Up-scaling flow in fractured media: equivalence between the large scale averaging theory and the continuous time random walk method, Transport Porous Media 43 (2001) 581–596.

[27] B. Wood, The role of scaling laws in upscaling, Adv. Water Resour. 32 (2009) 723–736.

[28] F. Golfier, M. Quintard, F. Cherblanc, C. Harvey, B. Zinn, B. Wood, Comparison of theory and experiment for solute transport in highly heterogeneous porous medium, Adv. Water Resour. 30 (11) (2007) 2225–2261.

[29] F. Howes, S. Whitaker, The spatial averaging theorem revisited, Chem. Eng. Sci. 40 (1985) 1387–1392.

[30] W. Gray, A. Leijnse, R. Kolar, C. Blain, Mathematical Tools for Changing Spatial Scales in the Analysis of Physical Systems, CRC Press, Boca Raton, FL, 1993.

[31] S. Whitaker, Introduction to Fluid Mechanics, R.E. Krieger, Malabar, FL, USA, 1981.

[32] A. Ahmadi, M. Quintard, S. Whitaker, Large-scale properties for two-phase flow in random porous media, J. Hydrol. 183 (1996) 69–99.

[33] P. Landereau, B. Noetinger, M. Quintard, Quasi-steady two-equation models for diffusive transport in fractured porous media: large-scale properties for densely fractured systems, Adv. Water Resour. 24 (2001) 863–876.

[34] F. Golfier, B. Wood, L. Orgogozo, M. Quintard, M. Buès, Biofilms in porous media: development of macroscopic transport equations via volume averaging with closure for local mass equilibrium conditions, Adv. Water Resour. 32 (2009) 463–485.

[35] B. Wood, S. Whitaker, Multi-species diffusion and reaction in biofilms and cellular media, Chem. Eng. Sci. 55 (2000) 3397–3418.

[36] A. Valocchi, Validity of the local equilibrium assumption for modeling sorbing phase solute transport through homogeneous soils, Water Resour. Res. 21 (1985) 808–820.

[37] C. Marle, P. Simandoux, J. Pacsirszky, C. Gaulier, Etude du déplacement de fluides miscibles en milieu poreux stratifié, Revue de l'Institut Francais du Pétrole 22 (1967) 272–294.

[38] Y. Davit, G. Debenest, B. Wood, M. Quintard, Modeling non-equilibrium mass transport in biologically reactive porous media, Adv. Water Resour., submitted for publication.

[39] H. Brenner, Dispersion resulting from flow through spatially periodic porous media, Philos. Trans. Royal Soc. London Ser. A 297 (1980) 81.

[40] H. Davarzani, M. Marcoux, M. Quintard, Theoretical predictions of the effective thermodiffusion coefficients in porous media, Int. J. Heat Mass Transfer 53 (2010) 1514–1528.